Macroscopic physical properties and spin dynamics in the layered superconductor $Fe_{1+\delta}Te_{1-x}Se_x$

Chishiro Michioka,[1,*] Hiroto Ohta,[1] Mami Matsui,[1] Jinhu Yang,[1] Kazuyoshi Yoshimura,[1,†] and Minghu Fang[2]
[1]*Department of Chemistry, Graduate School of Science, Kyoto University, Kyoto 606-8502, Japan*
[2]*Department of Physics, Zhejiang University, Hangzhou 310027, China*
(Received 7 January 2010; revised manuscript received 19 April 2010; published 10 August 2010)

Macroscopic physical properties of the novel layered superconducting system $Fe_{1+\delta}Te_{1-x}Se_x$ were investigated by means of magnetic-susceptibility, electric resistivity, and heat-capacity measurements. In addition to the substitution effect of the Te site, intercalated excess irons would suppress the bulk superconductivity. We have also performed ^{125}Te and ^{77}Se NMRs on a single crystal of $Fe_{1.04}Te_{0.67}Se_{0.33}$ with the highest superconducting transition temperature $T_c \sim 14$ K. In the superconducting state, the spin part of Knight shifts for both $H\|a$ and $H\|c$ are suppressed, and the nuclear-spin-lattice relaxation rate $1/T_1$ shows the power-law like behavior without any coherent peaks, indicating the nodal spin-singlet superconductivity. In the normal state, $1/T_1T$ is enhanced by antiferromagnetic spin fluctuations with decreasing temperature. The superconductivity in $Fe_{1+\delta}Te_{1-x}Se_x$ is realized in the vicinity of the magnetic quantum phase transition and is possibly mediated by the growth of the antiferromagnetic spin fluctuations.

DOI: 10.1103/PhysRevB.82.064506 PACS number(s): 74.70.Xa, 74.25.N−, 74.62.Dh, 74.78.Fk

I. INTRODUCTION

Since recent discoveries of iron-based superconductors with the superconducting transition temperature (T_c) being 55 K in the highest cases,[1–4] many studies have been done to search new materials with high T_c and to clarify the mechanism of superconductivity. In such investigations, the superconductivity was discovered with $T_c=8$ K in the α-FeSe system.[5] The α-FeSe has a simple layered structure in which the tetragonal FeSe layers stack continuously along the c axis without any insertions of another layers. Although the presence of Se defects is discussed in the report of the discovery of the superconductivity in FeSe,[5] Williams *et al.*[6] indicated that the stoichiometric FeSe is the most preferable for the superconductivity since the excess irons should suppress the superconductivity.[7] In the next stage, superconductivity in Se-substituted [the maximum $T_c=14$ K (Refs. 8 and 9)] and S-substituted [the maximum $T_c=10$ K (Ref. 10)] systems at the Te sites in FeTe, which is isostructural with the superconducting FeSe, were discovered. Fang *et al.*[8] presented that the end member α-FeTe shows a magnetic phase transition at 65 K, and the superconductivity of $FeTe_{1-x}Se_x$ occurs when the magnetic phase transition is suppressed by the increase in x. Because these Fe chalcogenide systems FeSe and $FeTe_{1-x}Se_x$ have the simplest structure with stacking in quasi-two-dimensional way, we can regard them as important key compounds to clarify the intrinsic properties of Fe-based superconductors.

In all the Fe-based superconductors, the superconductivity occurs in the vicinity of the magnetic phase. Therefore, the magnetic fluctuations are thought to play an important role in the Fe-based superconductors. NMR is a powerful method to investigate low-energy excitations of fluctuated spins. Imai *et al.*[11] presented that in almost stoichiometric FeSe, the relaxation rate divided by temperature ($1/T_1T$), which is proportional to the $\mathbf{q}$ summation of the imaginary part of the dynamical spin susceptibility $\mathrm{Im}\,\chi(\mathbf{q},\omega_N)/\omega_N$ at the NMR frequency ω_N, is enhanced at low temperatures. In a slightly Fe-rich $FeSe_{0.92}$ sample, the short T_1 component ($1/T_{1S}T$) also shows the enhancement with decreasing temperature together with the almost constant long T_1 component ($1/T_{1L}T$).[12,13] From a point of view of electronic spin fluctuations, Fe-based superconductors are grouped into two types: one shows the enhancement of $1/T_1T$ at low temperatures and the other does not show such the enhancement. The former group includes the 122-system (e.g., $Ba_{1-x}K_xFe_2As_2$) (Refs. 14–17) and the 11-system (e.g., FeSe),[11,13] and the latter the 1111-system (e.g., $LaFeAsO_{1-x}F_x$).[18–20] Even if there are some differences among each compound, it should be quite natural to consider that all the Fe-based superconductors have the same superconducting mechanism. It is, therefore, very important to investigate the spin fluctuations and the antiferromagnetic quantum criticality in the Fe-based superconductors.

The purpose of the present work is to clarify the role of spin fluctuations by studying the samples systematically from the antiferromagnetic FeTe to the superconducting $FeTe_xSe_{1-x}$. Since the Te site in the antiferromagnet FeTe can be substituted by Se over the whole composition range,[8,9] and furthermore, excess irons are doped in the other Fe site as nonstoichiometric $Fe_{1+\delta}Te_{1-x}Se_x$,[21–23] characterizations of the samples are very important.[24] In this paper we present the results of the magnetic susceptibility, heat capacity, and electric resistivity of the well characterized $Fe_{1+\delta}Te_{1-x}Se_x$, and those of ^{125}Te and ^{77}Se NMR studies in the single crystal $Fe_{1.04}Te_{0.67}Se_{0.33}$ which has the highest T_c.

II. EXPERIMENTAL

Single crystals of $Fe_{1+\delta}Te_{1-x}Se_x$ were prepared by the self-flux method in evacuated quartz tubes. Samples were characterized to be in a single phase by x-ray diffraction, and their compositions were measured by energy dispersive x-ray spectroscopy (EDS) using scanning electron microscope. The crystal axes were also determined from Laue photographs. The magnetic susceptibility χ was measured by using the superconducting quantum interference device magnetometer with the magnetic field parallel to the c axis. The elec-

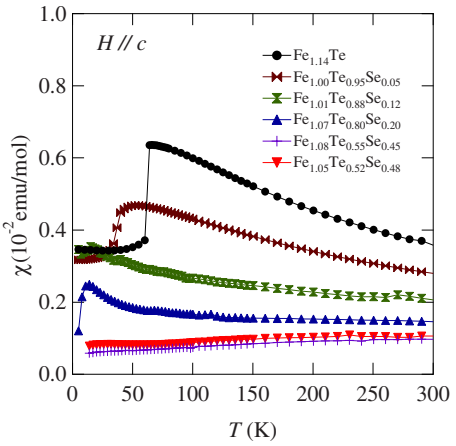

FIG. 1. (Color online) Temperature dependence of the magnetic susceptibility χ in $Fe_{1+\delta}Te_{1-x}Se_x$. The magnetic field is applied parallel to the c axis.

tric resistivity ρ was measured by the conventional four-probe method with a condition of electric currents and magnetic fields parallel to the a and c axes, respectively. The heat capacity was measured by the relaxation method up to 14 T. All the NMR measurements were carried out by spin-echo method with a standard phase-coherent-type pulsed NMR spectrometer. The magnetic fields were applied parallel to the a and c axes. NMR spectra were measured with sweeping magnetic field in a constant NMR frequency $\nu = \omega_N$. The Knight shift K is expressed as $K=(\nu_N/\gamma_N - H_{\rm res})/H_{\rm res}$, where γ_N and $H_{\rm res}$ are the nuclear gyromagnetic ratio and the resonance field, respectively. ^{125}Te and ^{77}Se nuclei with the nuclear spin $I=1/2$ have the nuclear gyromagnetic ratio $\gamma_N=13.454$ MHz/T and $\gamma_N=8.13$ MHz/T, respectively. The magnetic field was calibrated by reference signals of ^{2}D in D_2O and ^{125}Te in $TeCl_4$(aq). The nuclear-spin-lattice relaxation time (T_1) was measured by the inversion recovery method.

III. MACROSCOPIC PHYSICAL PROPERTIES

Figure 1 shows the temperature dependence of the magnetic susceptibility χ in $Fe_{1+\delta}Te_{1-x}Se_x$. In the sample with $x=0$, χ decreases rapidly at about 60 K with decreasing temperature. From the heat-capacity measurement, the first-order phase transition was found to occur at $T_N=61.5$ K. Below this temperature, the antiferromagnetic phase transition was confirmed by the ^{125}Te NMR measurement (not shown). With the increase in Se content x, T_N decreases and disappears above $x\sim0.2$, then superconductivity is observed with a maximum $T_c\sim14$ K. Among the samples with the maximum T_c, some samples show large superconducting volume fraction while other samples show poor one with an enhancement of χ in the normal state. This fact should not be attributed to the sample quality because all the single crystals are confirmed to be homogeneous by EDS and do not contain other impurity phases. Such an enhancement of χ is aroused by the moment of excess irons, whose $3d$ electrons were predicted to be almost localized from the result of the band calculation.[23] The amount of excess irons could hardly be

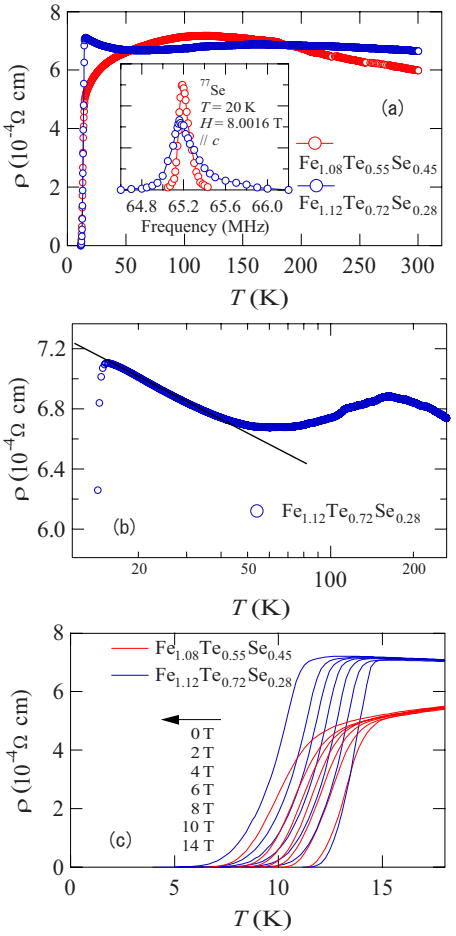

FIG. 2. (Color online) (a) Temperature dependence of the electric resistivity ρ in $Fe_{1.08}Te_{0.55}Se_{0.45}$ and $Fe_{1.12}Te_{0.72}Se_{0.28}$. Inset shows the ^{77}Se NMR spectra in the same samples with those used in the resistivity measurements. (b) ρ-T in semilogarithmic scale of $Fe_{1.12}Te_{0.72}Se_{0.28}$. (c) ρ-T in the magnetic field $H\|c$ up to 14 T.

characterized by the enhancement of χ or composition since there exist excess irons in $Fe_{1+\delta}Te_{1-x}Se_x$ system suggested by Williams *et al.*[6] as well as vacancies in the chalcogen site suggested by Hsu *et al.*[5] Excess irons would affect transport properties as well. Figure 2(a) shows the temperature dependence of the electric resistivities ρ of $Fe_{1.08}Te_{0.55}Se_{0.45}$ which does not show the enhancement of χ in the normal state and in $Fe_{1.12}Te_{0.72}Se_{0.28}$ which shows enhancement of χ due to the localized moments of excess irons. Both the samples show the superconductivity at about 14 K. Below 300 K, ρ of both samples increases slightly with decreasing temperature and decreases metallically below about 100 K. Therefore the electronic state probably changes gradually below 100 K. Just above T_c, ρ of $Fe_{1.12}Te_{0.72}Se_{0.28}$ again increases with decreasing temperature. Figure 2(b) shows ρ versus logarithmic scale of T in $Fe_{1.12}Te_{0.72}Se_{0.28}$. The ρ indicates the log T dependence, proving the impurity Kondo effect by the scattering between conduction electrons and nearly localized moments of excess irons. Figure 2(c) shows ρ-T under various magnetic fields H being parallel to the c axis. Compared with $Fe_{1.08}Te_{0.55}Se_{0.45}$, both the onset and zero resistivity T_c's in $Fe_{1.12}Te_{0.72}Se_{0.28}$ decrease rapidly with the increase in H.

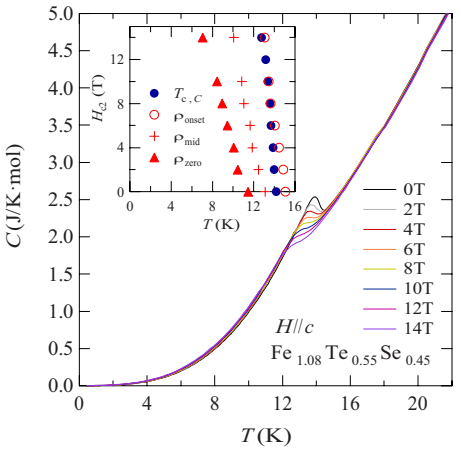

FIG. 3. (Color online) Temperature dependence of C in $Fe_{1.08}Te_{0.55}Se_{0.45}$ measured at various magnetic fields $H\|c$ up to 14 T. Inset shows the temperature dependence of H_{c2}.

This fact indicates that the localized magnetic moments of the excess irons disturb the formation of Cooper pairs, resulting in the suppression of the upper critical field (H_{c2}). From the sample dependence of the superconducting properties, it is also noted that all the samples with almost complete superconducting volume fractions do not show the enhancement of χ in the normal state but show the decrease in χ with decreasing temperature, which is consistent with the behavior of the Knight shift shown later. The inset in Fig. 2(a) shows the ^{77}Se NMR spectra in $Fe_{1.08}Te_{0.55}Se_{0.45}$ and $Fe_{1.12}Te_{0.72}Se_{0.28}$ measured at 20 K. The spectrum in the sample which shows the Kondo-effect like enhancement in resistivity has larger line width due to the excess irons. Such a tendency was observed in all the present NMR measurements.

Figure 3 shows the temperature dependence of the heat capacity C in $Fe_{1.08}Te_{0.55}Se_{0.45}$ measured under various magnetic fields H being parallel to the c axis up to 14 T. The inset shows the temperature dependence of H_{c2}, where $T_{c,C}$, ρ_{onset}, ρ_{mid}, and ρ_{zero} represent T_c determined from the minimum of $\frac{dC}{dT}$, the onset temperature in ρ-T, the middle point temperature in ρ-T, and the zero resistivity temperature in ρ-T, respectively. The initial slope of H_{c2} against T is quite large, suggesting the large H_{c2} at $T=0$ K. When one applies magnetic field being parallel to the a axis, the decrease in T_c is more slowly,[24] suggesting an anisotropic superconductivity. All the NMR measurements were performed under about 4 and 8 T in which T_c's are 13.87 and 13.56 K from the temperature dependence of the heat capacity, respectively. Since T_c at zero field is estimated as 14.19 K, the suppression of T_c by magnetic fields is less than 1 K in the present NMR measurements. Details of the heat capacity in the superconducting state is discussed later.

IV. MICROSCOPIC PROPERTIES AND SPIN DYNAMICS PROBED BY NMR

In the NMR measurements, we used a single crystal of $Fe_{1.04}Te_{0.67}Se_{0.33}$, in which the effect of excess irons is as small as in the sample used for the heat-capacity measurement. That of $Fe_{1.12}Te_{0.72}Se_{0.28}$ with small superconducting volume fraction was also used for comparison.

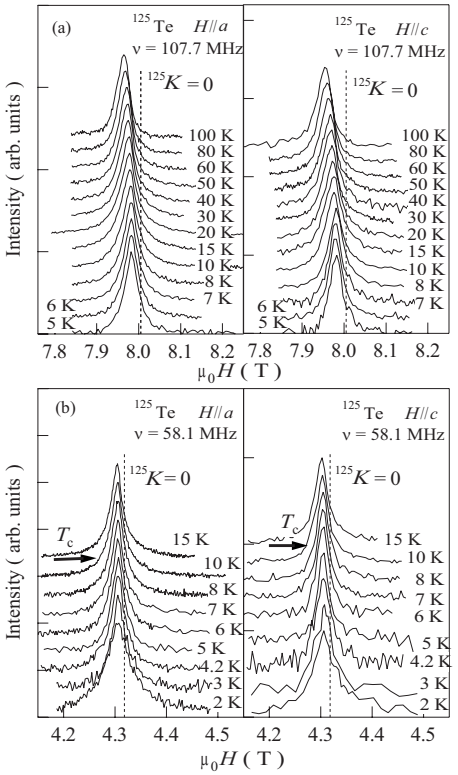

FIG. 4. Field-swept ^{125}Te NMR spectra in $Fe_{1.04}Te_{0.67}Se_{0.33}$ at constant frequencies (a) ν_N=107.7 MHz and (b) ν_N=58.1 MHz with magnetic fields H parallel to the a and c axes.

Figures 4(a) and 4(b) show the field-swept ^{125}Te NMR spectra in the normal state with a constant frequency ν_N =107.7 MHz (corresponding to $\nu_N/\gamma_N \sim 8$ T) and those in the superconducting state with ν_N=58.1 MHz (corresponding to $\nu_N/\gamma_N \sim 4.3$ T) in $Fe_{1.04}Te_{0.67}Se_{0.33}$. In both conditions of $H\|a$ and $H\|c$, the peak fields of the spectra increase with decreasing temperature. The linewidth is about three times larger than that in $Fe_{1.01}Se$,[11] indicating distribution of the local surroundings around Te sites due to the Se substitution and the presence of excess irons. In the case of $Fe_{1.12}Te_{0.72}Se_{0.28}$, the linewidth of the NMR spectrum is much larger than that in $Fe_{1.04}Te_{0.67}Se_{0.33}$. The increase in the amount of excess irons would enlarge the chemical distribution around the Te site. In the superconducting state, the peak fields for both $H\|a$ and $H\|c$ increase slightly with the decrease in temperature as well as in the normal state. Below T_c the spin-echo intensity of the NMR spectrum is markedly weakened and the linewidth of the spectrum increases with decreasing temperature. At 4.2 K the estimated Knight shift at resonance center of the field-swept spectrum agrees with that of the frequency-swept spectrum. In the present stage, we cannot estimate demagnetization. Therefore, we can roughly discuss the behavior of Knight shift but cannot do details of the vortex state.

Figure 5 shows the temperature dependence of the Knight shift of ^{125}Te NMR (^{125}K) in $Fe_{1.04}Te_{0.67}Se_{0.33}$ with the Knight shift of ^{77}Se NMR (^{77}K) for comparison. In the nor-

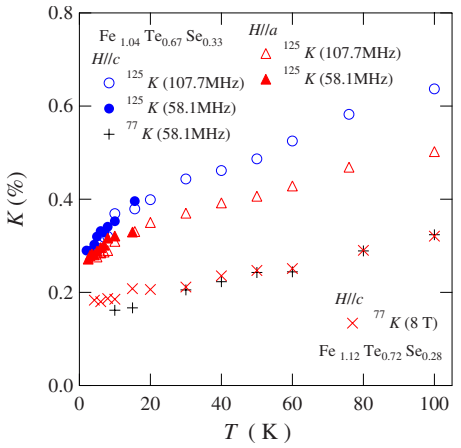

FIG. 5. (Color online) Temperature dependence of Knight shifts, ^{125}K and ^{77}K in $Fe_{1.04}Te_{0.67}Se_{0.33}$ and ^{77}K in $Fe_{1.12}Te_{0.72}Se_{0.28}$.

mal state, both ^{125}K and ^{77}K decrease with decreasing temperature, similar to the case with $Fe_{1.01}Se$.[11] In $Fe_{1.04}Te_{0.67}Se_{0.33}$, both ^{125}K and ^{77}K are well scaled with χ. On the other hand, χ in $Fe_{1+\delta}Te_{1-x}Se_x$ with large δ shows an enhancement in the normal state. However, in $Fe_{1.12}Te_{0.72}Se_{0.28}$ which is one of such compounds Knight shift decreases with decreasing temperature as well as that in $Fe_{1.04}Te_{0.67}Se_{0.33}$. Therefore, the hyperfine coupling constant between the chalcogen nuclear spin and the localized moment of excess irons is small. In the NMR spectroscopy at chalcogen sites, excess irons mainly affect the linewidth. The suppression of the uniform spin susceptibility with decreasing temperature was found in many itinerant antiferromagnets[11,25,26] similar to the present case, which is consistent with the presence of antiferromagnetic spin fluctuations probed by $1/T_1T$ shown below.

Figure 6 shows Knight shifts plotted against the uniform susceptibility (so-called K-χ plot) for ^{125}Te and ^{77}Se in $Fe_{1.04}Se_{0.33}Te_{0.67}$ with temperature as an implicit parameter. As discussed above, when the amount of excess irons is small, χ does not show the enhancement and decreases with

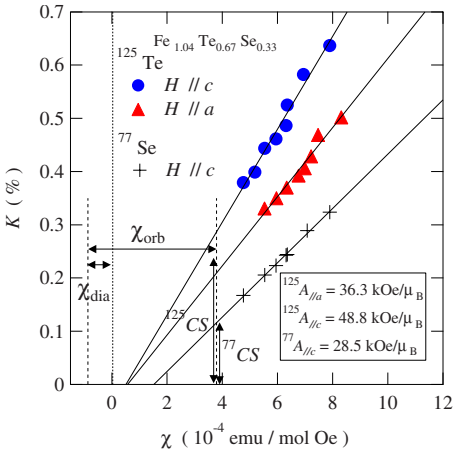

FIG. 6. (Color online) Knight shifts ^{77}K and ^{125}K plotted against the uniform susceptibility χ in $Fe_{1.04}Te_{0.67}Se_{0.33}$. χ_{dia}, χ_{orb}, ^{77}CS, and ^{125}CS denote diamagnetic and orbital contributed χ and chemical shifts of ^{77}Se and ^{125}Se nuclei, respectively.

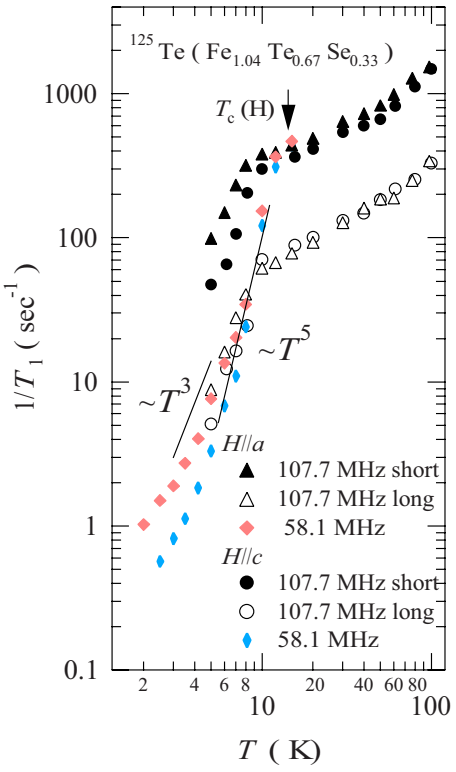

FIG. 7. (Color online) Temperature dependence of the nuclear-spin-lattice relaxation rate $(1/T_1)$ of ^{125}Te in $Fe_{1.04}Te_{0.67}Se_{0.33}$. At ν=58.1 MHz (~4.3 T), below T_c the main part of $1/T_1$ shows rapid decrease obeying $\sim T^n$ law without any coherence peaks, indicating the possible nodal superconducting gap (see text).

decreasing temperature similar to K. The K-χ plots show good linearities as seen in Fig. 6. The temperature dependent K and χ originate in the spin parts of them. From the slopes, hyperfine coupling constants due to electronic spins can be estimated as $^{125}A_{\|a}$=36.3 kOe/μ_B, $^{125}A_{\|c}$=48.8 kOe/μ_B, and $^{77}A_{\|c}$=28.5 kOe/μ_B. Next, we should discuss the temperature-independent terms of K and χ. In general, the chemical shift of ^{125}Te is very large, sometimes up to 0.3%, and is by a factor of ~2 larger than that of ^{77}Se when they are located in the same chemical surroundings.[27] From the ratio of chemical shifts of ^{125}Te and ^{77}Se in the same site, we can roughly estimate the chemical shifts in $Fe_{1.04}Se_{0.33}Te_{0.67}$ as $^{125}CS \sim 0.25\%$ and $^{77}CS \sim 0.12\%$, and then χ_{orb} can be estimated as $\sim 4.5 \times 10^{-4}$ emu/mol as shown in Fig. 6.

In the superconducting state as shown in Fig. 5, both $^{125}K_a$ and $^{125}K_c$ decrease with decreasing temperature. From the roughly estimated chemical shifts in $Fe_{1.04}Se_{0.33}Te_{0.67}$, the spin contributed Knight shift K_{spin} seems to be completely suppressed in the ground state for both magnetic field directions, although there remain ambiguities due to the effects of the demagnetization and chemical shift. The similar decreasing behavior in both $^{125}K_a$ and $^{125}K_c$ possibly suggests the spin-singlet superconductivity. Since the spectral shape changes at low temperatures, we need detailed studies at various constant fields for further discussion.

Figure 7 shows the temperature dependence of the ^{125}Te nuclear-spin-lattice relaxation rate $(1/T_1)$ in $Fe_{1.04}Te_{0.67}Se_{0.33}$ for both conditions of $H\|a$ and $H\|c$. Since the recovery of

the nuclear-spin momentum cannot be fitted by the function with the single T_1 component, the recovery curves were fitted by the relaxation function with the sum of long and slow T_1 components, as follows:

$$\frac{M(\infty)-M(t)}{M(\infty)} = p_{0S}\exp\left(\frac{-t}{T_{1S}}\right) + p_{0L}\exp\left(\frac{-t}{T_{1L}}\right), \qquad (1)$$

where p_{0S}, p_{0L}, T_{1S}, and T_{1L} are fitting parameters. This situation is similar to the case with $FeSe_{0.92}$ (Ref. 13) while nearly stoichiometric $Fe_{1.01}Se$ does not show any distributions of T_1.[11] In the case of $Fe_{1.04}Te_{0.67}Se_{0.33}$, the main part of the recovery is attributed to the short T_1 component with a fraction of ~80%. On the other hand, in the case of $Fe_{1.12}Te_{0.72}Se_{0.28}$ the fraction of the long component is larger than that in $Fe_{1.04}Se_{0.33}Te_{0.67}$, resulting in that the increase in the amount of excess irons may increase the fraction of long T_1 component with the enlargement of the spectral linewidth. In the superconducting state, we also measured T_1 at lower field ($H \sim 4.3$ T). The recovery curves below T_c have large distribution of T_1 due to contributions both from superconducting and vortex sites, and cannot be fitted by long and short two components. In these regions, we estimated T_1 from the main component of the recovery curves, i.e., we determined T_1 at the region where recovery curve can be fitted by the single exponential in the longest time region of two digits recovering. The estimated T_1 below 8 K is the slowest component which should come from the intrinsic superconductivity.

In the normal state, the relaxation rates of both short and long T_1 components, $1/T_{1S}$ and $1/T_{1L}$, decrease with decreasing temperature, and the anisotropy is small. For the main short T_1 component, $1/T_{1S,H\|a}$ is about 20% larger than $1/T_{1S,H\|c}$. $1/T_{1S,H\|a}$ and $1/T_{1S,H\|c}$ are proportional to $(\delta h_a)^2 + (\delta h_c)^2$ and $(\delta h_a)^2 + (\delta h_a)^2$, respectively, where $\delta h_{a,c}$ are local magnetic fluctuations. Taking it into account that $^{125}A_{\|c}$ is larger than $^{125}A_{\|a}$, the anisotropy of $1/T_{1S}$ can be qualitatively explained by the anisotropy of the hyperfine coupling constants estimated from K-χ plots.

In the superconducting state, theoretically $1/T_1$ decreases proportional to $\sim T^3$ and $\sim T^5$ in the presence of line and point nodes in the superconducting gap, respectively. In the case of $Fe_{1.04}Se_{0.33}Te_{0.67}$, below T_c the $1/T_1$ decreases proportional to $\sim T^5$ near T_c without any coherent peaks, then decreases as $\sim T^n$ with smaller index of n, resulting in an unconventional superconductiving state possibly with the nodal gap. Although in the present stage, we cannot elucidate the behavior of $1/T_1$ uniquely due to an ambiguity of the fitting of the recovery curves as well as poor information of the field dependence, detailed analysis of the heat capacity help us for further understanding of the superconducting symmetry as shown below. At low temperatures, the slope of $1/T_1$ seems to be close to T linear due to the residual density of state. Such a behavior often appears in the case of unconventional superconductors because even nonmagnetic impurity scatterings can easily break Cooper pairs, except for the electron-phonon coupling case of the BCS type.

Figure 8 shows the temperature dependence of the electron contributed heat capacity. The inset shows the heat capacity divided by temperature plotted against the T square. In the normal state, the data can be fitted linearly between 15 and 20 K. The electron specific-heat coefficient γ is estimated as 96.3 mJ/K^2 mol. The large γ suggests the strong electron-electron correlation. In the superconducting state, the electron contributed heat capacity was estimated with an assumption that the phonon contribution to the heat capacity C_{ph} is unchanged as βT^3, where β is a constant associated with the Debye temperature. Just below T_c the electron contributed heat capacity $(C - C_{ph})$ at zero field decreases as $\sim T^n$ with $n \sim 3$, then decreases with smaller n, finally T-linear behavior was observed at very low temperatures. Taking into account the fact that the electron contributed heat capacity obeys nearly T^2 and T^3 laws in the cases of the line and point nodal gaps, respectively, $1/T_1$ and $C - C_{ph}$ are attributed to the same low-energy excitations in the superconducting state. Although the presence of the point node seems to be most preferable, in the present stage we cannot determine the symmetry of the superconducting gap and cannot rule out the possibility of multiple-gap and/or anisotropic $s_{\pm}$-wave scenarios.[28] In $Ba_{0.6}K_{0.4}Fe_2As_2$, the similar behavior of $1/T_1$ was observed below T_c, i.e., $1/T_1$ decreases rapidly just below T_c without any coherence peaks, then the slope gradually changes at low temperatures.[29]

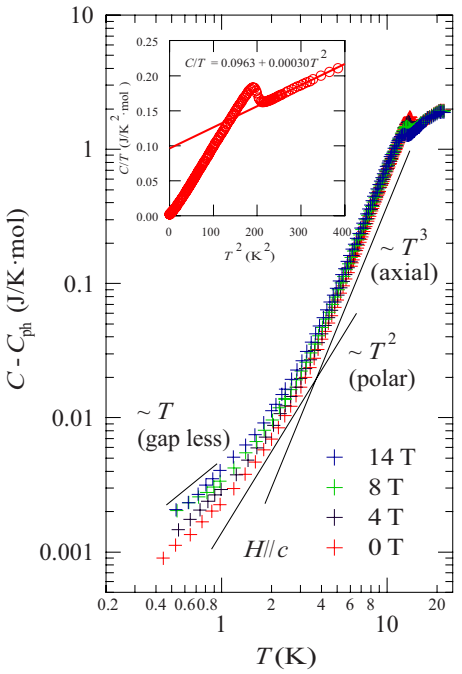

FIG. 8. (Color online) Temperature dependence of the electron contributed heat capacity in $Fe_{1.08}Te_{0.55}Se_{0.45}$. Inset shows the heat capacity divided by temperature C/T plotted against T^2.

Figure 9 shows the temperature dependence of the nuclear-spin-lattice relaxation rate divided by temperature $(1/T_1T)$ of ^{125}Te in $Fe_{1.04}Te_{0.67}Se_{0.33}$. In both conditions of $H\|a$ and $H\|c$, both $1/T_{1S}$ and $1/T_{1L}$ are enhanced with the decrease in temperature. Generally, $1/T_1T$ is proportional to $\Sigma_{\mathbf{q}}|A_{hf}(\mathbf{q})|^2 \mathrm{Im}\,\chi(\mathbf{q},\omega_N)/\omega_N$, where $A_{\mathbf{q}}$ is the $\mathbf{q}$ dependent hyperfine coupling constant, ω_N the NMR frequency, and $\mathrm{Im}\,\chi(\mathbf{q},\omega_N)$ the imaginary part of the dynamical spin susceptibility at ω_N.[30] The enhancement of $1/T_1T$ is attributed to

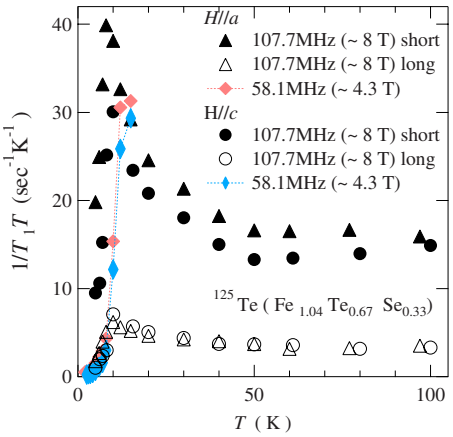

FIG. 9. (Color online) Temperature dependence of the nuclear-spin-lattice relaxation rate divided by temperature $(1/T_1T)$ for ^{125}Te in $Fe_{1.04}Te_{0.67}Se_{0.33}$.

the development of Im $\chi(\mathbf{q},\omega_N)$. The enhancement of $1/T_1T$ was also observed in $Fe_{1.01}Se$.[11] Shimizu *et al.*[31] reported that in a powder sample of $FeSe_{0.5}Te_{0.5}$, $1/T_1T$ decreases with decreasing temperature at ambient pressure in the normal state while $1/T_1T$ shows an enhancement at high pressure of 2 GPa. Our data in $Fe_{1.04}Te_{0.67}Se_{0.33}$ are similar to the case at 2 GPa but not at ambient pressure in $FeSe_{0.5}Te_{0.5}$. It might be due to an effect of powder summation of the anisotropic recovery curves or the effect of excess irons.

In the report of neutron-diffraction measurements, an incommensurate $(\delta\pi,\delta\pi)$ short-range magnetic ordering was observed even in the superconducting $Fe_{1.080}Te_{0.67}Se_{0.33}$, and δ can be tunable with the amount of excess irons.[22] The spin fluctuations with incommensurate $\mathbf{q}$ are expected to give a finite $A(\mathbf{q})$ at any crystal sites. Therefore, the enhancement of $1/T_1T$ in the present result may probe the similar spin fluctuations by neutron diffraction. In the case of $Fe_{1.12}Te_{0.72}Se_{0.28}$, the absolute value of $1/T_1T$ is smaller than that in $Fe_{1.04}Te_{0.67}Se_{0.33}$, suggesting that excess irons may suppress the antiferomagnetic spin fluctuations, which mediate pair electrons in the superconductiving state. By the density function calculations, the curious valence state Fe^+ is predicted to occur in the excess iron sites, i.e., the Fe(II) sites in $Fe_{1+\delta}Te$ with nearly localized strong magnetic moments.[23] The role of excess irons is not only pair breaking by magnetic scattering at the superconducting state but also change the electronic state by the carrier doping effect. Since the superconductivity is strongly related to the magnetic instability, the magnetic fluctuations proved by $1/T_1T$ are thought to be the driving force and the origin of superconductivity in the present Fe-based system.

V. CONCLUSIONS

We presented systematic macroscopic physical properties of $Fe_{1+\delta}Te_{1-x}Se_x$. The excess irons were found to work as magnetic impurities and to suppress the upper critical field H_{c2}. We also measured ^{125}Te NMR on the single crystal of $Fe_{1.04}Se_{0.33}Te_{0.67}$ and found possibly the nodal superconducting gap with the spin-singlet superconducting pairing. The results of $1/T_1$ of ^{125}Te were confirmed to be consistent with the results of heat-capacity measurements. We also found that the magnetic fluctuations derived from $1/T_1T$ have an important role for the occurrence of the superconductivity in the present Fe chalcogenide system.

ACKNOWLEDGMENTS

This work was supported by Grants-in-Aid for Scientific Research on Priority Area "Invention of anomalous quantum materials," from the Ministry of Education, Culture, Sports, Science and Technology of Japan (Grant No. 16076210) and also by Grants-in-Aids for Scientific Research from the Japan Society for Promotion of Science (Grants No. 19350030 and No. 22350029). The works at Zejiang University were supported by the National Science Foundation of China (Grants No. 10974175, No. 10874146, and No. 10934005), the National Basic Research Program of China (Grant No. 2009CB929104), and the PCSIRT of the Ministry of Education of China (Grant No. IRT0754).

*michioka@kuchem.kyoto-u.ac.jp
†kyhv@kuchem.kyoto-u.ac.jp

[1] Y. Kamihara, T. Watanabe, M. Hirano, and H. Hosono, J. Am. Chem. Soc. **130**, 3296 (2008).
[2] Z. A. Ren, W. Lu, J. Yang, W. Yi, X. L. Shen, Z. C. Li, G. C. Che, X. L. Dong, L. L. Sun, F. Zhou, and Z. X. Zhao, Chin. Phys. Lett. **25**, 2215 (2008).
[3] X. F. Chen, T. Wul, G. Wu, R. H. Liu, H. Chen, and D. F. Fang, Nature (London) **453**, 761 (2008).
[4] H. Kito, H. Eisaki, and A. Iyo, J. Phys. Soc. Jpn. **77**, 063707 (2008).
[5] F. C. Hsu, J. Y. Luo, K. W. Yeh, T. K. Chen, T. W. Huang, P. W. Wu, Y. C. Lee, Y. L. Huang, Y. Y. Chu, D. C. Yan, and M. K. Wu, Proc. Natl. Acad. Sci. U.S.A. **105**, 14262 (2008).
[6] A. J. Williams, T. M. McQueen, and R. J. Cava, Solid State Commun. **149**, 1507 (2009).
[7] T. M. McQueen, Q. Huang, V. Ksenofontov, C. Felser, Q. Xu, H. Zandbergen, Y. S. Hor, J. Allred, A. J. Williams, D. Qu, J. Checkelsky, N. P. Ong, and R. J. Cava, Phys. Rev. B **79**, 014522 (2009).
[8] M. H. Fang, H. M. Pham, B. Qian, T. J. Liu, E. K. Vehstedt, Y. Liu, L. Spinu, and Z. Q. Mao, Phys. Rev. B **78**, 224503 (2008).
[9] K. W. Yeh, T. W. Huang, Y. L. Huang, T. K. Chen, F. C. Hsu, Phillip M. Wu, Y. C. Lee, Y. Y. Chu, C. L. Chen, J. Y. Luo, D. C. Yang, and M. K. Wu, EPL **84**, 37002 (2008).
[10] Y. Mizuguchi, F. Tomioka, S. Tsuda, T. Yamaguchi, and Y. Takano, Appl. Phys. Lett. **94**, 012503 (2009).
[11] T. Imai, K. Ahilan, F. L. Ning, T. M. McQueen, and R. J. Cava, Phys. Rev. Lett. **102**, 177005 (2009).
[12] H. Kotegawa, S. Masaki, Y. Awai, H. Tou, Y. Mizuguchi, and Y.

Takano, J. Phys. Soc. Jpn. **77**, 113703 (2008).
[13] S. Masaki, H. Kotegawa, Y. Hara, H. Tou, K. Murata, Y. Mizuguchi, and Y. Takano, J. Phys. Soc. Jpn. **78**, 063704 (2009).
[14] S.-H. Baek, H. Lee, S. E. Brown, N. J. Curro, E. D. Bauer, F. Ronning, T. Park, and J. D. Thompson, Phys. Rev. Lett. **102**, 227601 (2009).
[15] H. Fukazawa, Y. Yamada, K. Kondo, T. Saito, Y. Kohori, K. Kuga, Y. Matsumoto, S. Nakatsuji, H. Kito, P. M. Shirage, K. Kihou, N. Takeshita, C.-H. Lee, A. Iyo, and H. Eisaki, J. Phys. Soc. Jpn. **78**, 083712 (2009).
[16] F. Ning, K. Ahilan, T. Imai, A. S. Sefat, R. Jin, M. A. McGuire, B. C. Sales, and D. Mandrus, J. Phys. Soc. Jpn. **77**, 103705 (2008).
[17] F. Ning, K. Ahilan, T. Imai, A. S. Sefat, R. Jin, M. A. McGuire, B. C. Sales, and D. Mandrus, J. Phys. Soc. Jpn. **78**, 013711 (2009).
[18] Y. Nakai, K. Ishida, Y. Kamihara, M. Hirano, and H. Hosono, J. Phys. Soc. Jpn. **77**, 073701 (2008).
[19] Y. Nakai, S. Kitagawa, K. Ishida, Y. Kamihara, M. Hirano, and H. Hosono, Phys. Rev. B **79**, 212506 (2009).
[20] H. Mukuda, N. Terasaki, N. Tamura, H. Kinouchi, M. Yashima, Y. Kitaoka, K. Miyazawa, P. M. Shirage, S. Suzuki, S. Miyasaka, S. Tajima, H. Kito, H. Eisaki, and A. Iyo, J. Phys. Soc. Jpn. **78**, 084717 (2009).
[21] D. Fruchart, P. Convert, P. Wolfers, R. Madar, J. P. Senateur, and R. Frucart, Mater. Res. Bull. **10**, 169 (1975).
[22] Wei Bao, Y. Qiu, Q. Huang, M. A. Green, P. Zajdel, M. R. Fitzsimmons, M. Zhernenkov, S. Chang, M. Fang, B. Qian, E. K. Vehstedt, J. Yang, H. M. Pham, L. Spinu, and Z. Q. Mao, Phys. Rev. Lett. **102**, 247001 (2009).
[23] L. Zhang, D. J. Singh, and M. H. Du, Phys. Rev. B **79**, 012506 (2009).
[24] J. Yang, M. Matsui, M. Kawa, H. Ohta, C. Michioka, C. Dong, H. Wang, H. Yuan, M. Fang, and K. yoshimura, J. Phys. Soc. Jpn. **79**, 074704 (2010).
[25] D. C. Johnston, Phys. Rev. Lett. **62**, 957 (1989).
[26] M. Takigawa, A. P. Reyes, P. C. Hammel, J. D. Thompson, R. H. Heffner, Z. Fisk, and K. C. Ott, Phys. Rev. B **43**, 247 (1991).
[27] Chemical shifts in ^{77}Se and ^{125}Te NMR are, for example, investigated in B. A. Denko and E. Wasylishen, Prog. Nucl. Magn. Reson. Spectrosc. **54**, 208 (2009); M. Biil, W. Thiel, U. Fleischer, and W. Kutzelnigg, J. Phys. Chem. **99**, 4000 (1995); H. Nakatsuji, T. Higashioji, and M. Sugimoto, Bull. Chem. Soc. Jpn. **66**, 3235 (1993); M. Hada, J. Wan, R. Fukuda, and H. Nakatsuji, J. Comput. Chem. **22**, 1502 (2001); S. Sakida, S. Hayakawa, and T. Yoko, J. Non-Cryst. Solids **243**, 1 (1999).
[28] Y. Nagai, N. Hayashi, N. Nakai, H. Nakamura, M. Okumura, and M. Machida, New J. Phys. **10**, 103026 (2008).
[29] H. Fukazawa, T. Yamazaki, K. Kondo, Y. Kohori, N. Takeshita, P. M. Shirage, K. Kihou, K. Miyazawa, H. Kito, H. Eisaki, and A. Iyo, J. Phys. Soc. Jpn. **78**, 033704 (2009).
[30] T. Moriya, J. Phys. Soc. Jpn. **18**, 516 (1963).
[31] Y. Shimizu, T. Yamada, T. Takami, S. Niitaka, H. Takagi, and M. Itoh, J. Phys. Soc. Jpn. **78**, 123709 (2009).